Supporting Information

Identification of new P300 acetyltransferase inhibitors from natural products by a customized virtual screening method

Guo-Bo Li,[a] Lu-Yi Huang,[a] Hui Li,[a] Sen Ji,[a] Lin-Li Li,[b] and Sheng-Yong Yang[a,*]

[a] *State Key Laboratory of Biotherapy/Collaborative Innovation Center for Biotherapy, West China Hospital, West China Medical School, Sichuan University, Sichuan 610041, China*

[b] *Key Laboratory of Drug Targeting and Drug Delivery System of Ministry of Education, West China School of Pharmacy, Sichuan University, Chengdu, Sichuan, 610041, China*

* to whom correspondence should be addressed. Tel.: +86-28-85164063; Fax: +86-28-85164060. E-mail: yangsy@scu.edu.cn.

CONTENT

Experimental Methods.

Customized Virtual Screening Procedures. On the basis of the hypothesis that essential pharmacophore features for potent p300 HAT inhibitor are hydrogen-bonds with residues Arg1410, Thr1411, and Trp1466, we established a target-customized structure-based virtual screening method to screen potential hits from natural product libraries. All the chemical structures of natural products commercially available in Specs Natural Products, AnalytiCon Discovery Natural Products, Indofine Natural Products, and Princeton Natural Products were downloaded from ZINC database because they are well prepared for docking. This first step is to use three rules including (i) molecule weight ≤ 500, (ii) number of polar atoms ≤ 10, and (iii) number of rotatable bonds ≤ 10 to filter the collected natural products to exclude the large complicated compounds by an in-house program derived from our previously programs. The second step uses Autodock vina to predict the binding modes and affinities for the filtered compounds from the first step. The crystal structure of p300 HAT in complex with Lys-CoA (PDB entry: 3BIY) was used as the docking template. Gasteiger-Marsili charges were added to the models of protein and compounds, and then non-polar hydrogens were merged onto their respective heavy atoms using AutoDockTools and Raccoon. The grid center was set as the co-crystal ligand Lys-CoA (x, y, z = -17.628, 15.959, 1.475), and the grid size was 26Å × 26Å × 26Å, which encompassed the entire p300 HAT binding site. The other parameters for Vina were set as default. The third step uses hydrogen-bonding

analysis to analyse the docking poses using an in-house program. The hydrogen bonds were defined as the same with that described in ID-Score method[1], and only the compounds likely to form hydrogen-bonds with the three key residues were kept. The final step is manually visualisation to confirm whether or not the predicted binding poses are reasonable. Using this customized virtual screening protocol, we performed a screening campaign against 28,969 natural compounds, and obtained 110 potential hit compounds for p300 HAT (see Supporting Information Table S1).

Enzymatic Inhibitory Assays. Natural compounds **NP-1** to **NP-15** were purchased from Specs company and used without further purification. p300 HAT inhibitory assays were performed using labelled 3H-Ac-CoA and substrate peptide by Shanghai ChemPartner Co., Ltd. The purchased materials include p300 (BPS, Cat. No. 50071), 3H-Ac-CoA (PerkinElmer, Cat. No. NET290), Ac-CoA (Sigma, Cat. No. A2056), C646 (Calbiochem, Cat. No. 382113), and 384-well Flashplate (Perkin Elmer, Cat. No. SMP410A001PK). The assay buffer is modified Tris buffer, and the substrate is H3 peptide. The reaction is initiated by the addition of 10 μL the substrate solution. After incubation of 60 mins at room temperature, the reaction was stopped by adding 10 μL stop solution. Volume of 25 μL reaction solutions are transferred to Flashplate, and incubated for 1 hour, and washed three times using dH_2O and 0.1% Tween-20 prior to reading on Microbeta. The inhibition activity is calculated according to the equation: Inh% = (Max-Signal)/(Max-Min)*100. All the assays were replicated twice, and the

means of the replicates were calculated. The IC_{50} values were determined from dose-response curves using Graphpad Prism 5 after carrying out assays at 10 different concentrations for each compound.

The inhibitory activities of **NP-2**, **NP-3**, **NP-9** and **NP-15** against the other three histone acetylases including PCAF, KAT1, and HAT7 were also carried out by ChemPartner Co., Ltd. The purchased materials include PCAF (Cayman, Cat. No. 10009115), HAT1 (Prospec, Cat. No. enz-504), and KAT7 (Active Motif). The screening protocols for PCAF, KAT1, and HAT7 as well as the calculation method for inhibition activity are the same as that described above for p300 HAT assays. All the assays were replicated twice, and the means of the replicates were calculated. The IC_{50} values of **NP-2**, **NP-3**, **NP-9** and **NP-15** for PCAF were determined from dose-response curves using Graphpad Prism 5 after carrying out assays at 10 different concentrations.

Cell lines. All cell lines used were obtained from American Type Culture Collection (ATCC). These cell lines were cultured in culture medium supplemented with 10% FBS (Caoyuanlvye). All cell lines were maintained at 37 °C in a CO_2 incubator with 5% CO_2.

Cell viability assay. Effects of compounds on the cell viability of tumor cell lines were examined using a cell viability reagent, MTT (Sigma). Briefly, tumor cells were seeded in a 96-well plate in the absence or presence of tested natural compounds for 96 h. MTT (5 mg/ml in sodium chloride) was added for the last

3 h of incubation, and the absorbances at 570 nm were measured after the dissolve of 20% SDS. The IC_{50} values were calculated by GraphPad Prism 5.01 software (GraphPad Software, USA).

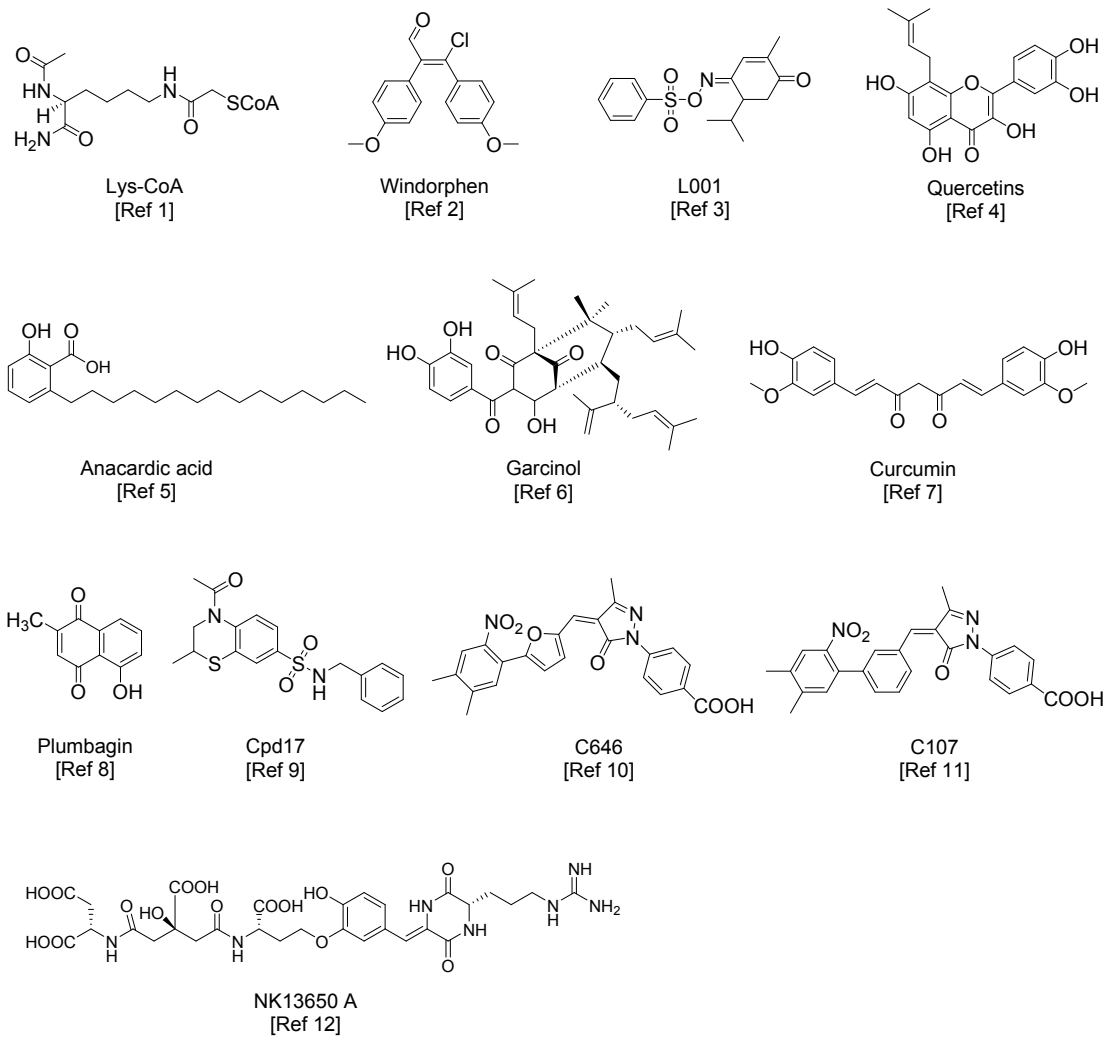

Fig. S1. Chemical structures of known P300 HAT inhibitors[2-13].

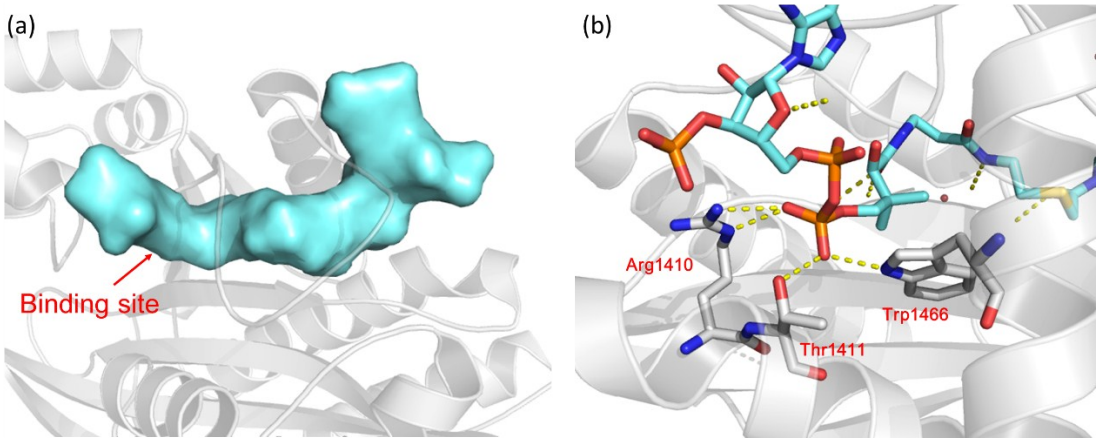

Fig. S2. P300 HAT binding site shape and the key binding feature for substrate Acetyl-CoA. (a) P300 HAT binding site shape, and (b) The key binding feature for substrate Acetyl-CoA which is having hydrogen-bonds with Arg1410, Thr1411, and Trp1466.

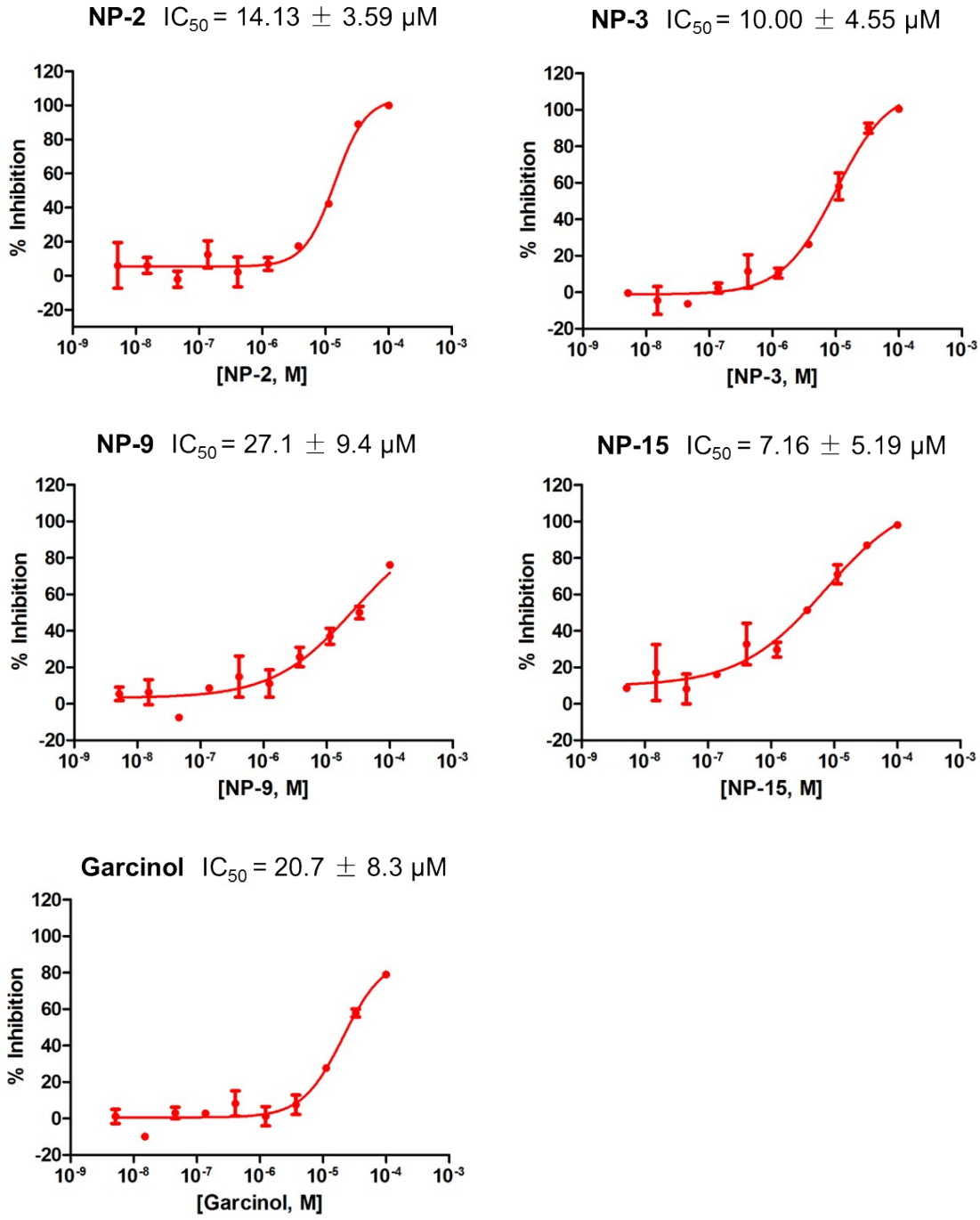

Figure S3. The IC_{50} curves of compounds **NP-2**, **NP-3**, **NP-9**, **NP-15**, and positive control, the known PCAF inhibitor Garcinol (IC_{50} values were reported as *mean* ± *SD*).

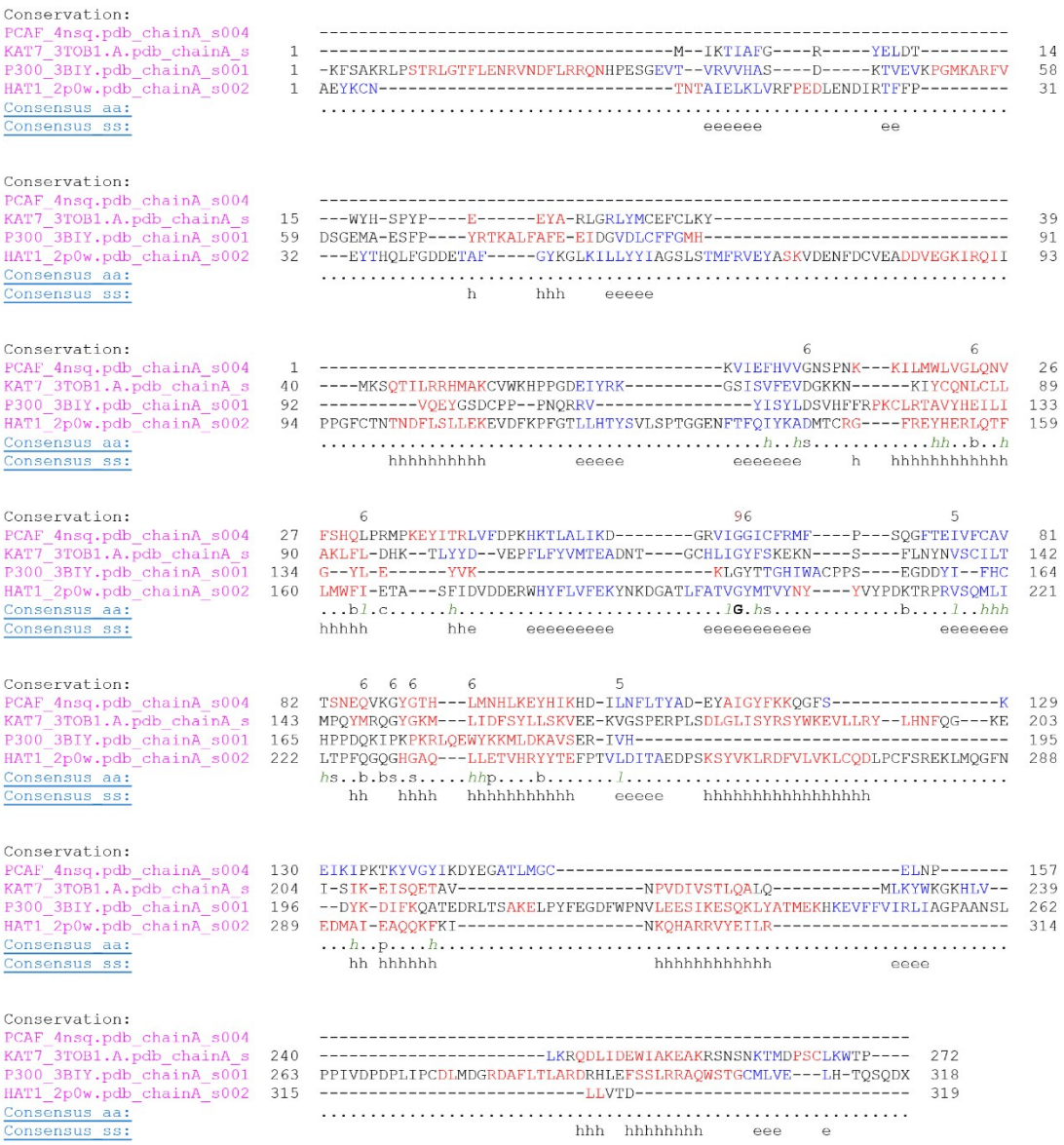

Figure S4. Colored alignment with secondary structure, conservation, and consensus sequence information of p300, PCAF, HAT1, and KAT7 using PROMALS3D[14]. The last two lines show consensus amino acid sequence (Consensus_aa) and consensus predicted secondary structures (Consensus_ss). Representative sequences have magenta names and they are colored according to predicted secondary structures (red: alpha-helix, blue: beta-strand). Consensus predicted secondary structure symbols: alpha-helix: h; beta-strand: e. Consensus amino acid symbols are: conserved amino acids are in bold and uppercase letters; aliphatic (I, V, L): l; aromatic (Y, H, W, F): @; hydrophobic (W, F, Y, M, L, I, V, A, C, T, H): h; alcohol (S, T): o; polar residues (D, E, H, K, N, Q, R, S, T): p; tiny (A, G, C, S): t; small (A, G, C, S, V, N, D, T, P): s; bulky residues (E, F, I, K, L, M, Q, R, W, Y): b; positively charged (K, R, H): +; negatively charged (D, E): -; charged (D, E, K, R, H): c.

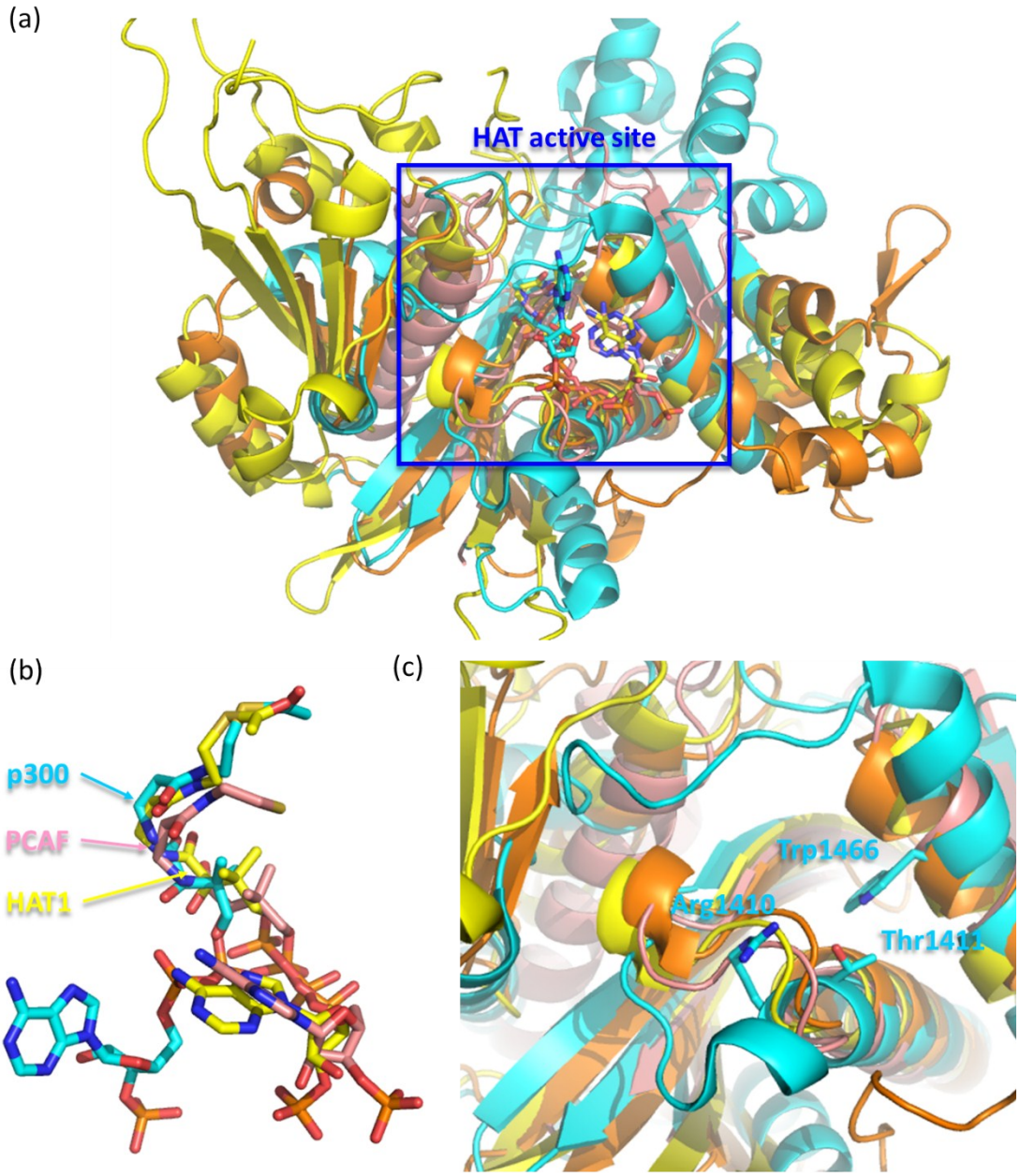

Figure S5. Comparison of tertiary structure, substrate, and key residues of p300, PCAF, HAT1, and KAT7. (a) Alignment of crystal structures of the HAT domain of p300 (PDB code: 4PZS, blue), PCAF (PDB code: 4NSQ, pink), and HAT1 (PDB code: 2P0W, yellow), and the predicted KAT7 HAT domain (orange) using the MICAN program[15], indicating the active site of p300 HAT is significantly different from that of PCAF, HAT1, and KAT7 in protein tertiary structure; (b) The co-crytal substrates (acetyl-CoA or CoA) extracted from (a), the alignment of tertiary structures, showing a significant difference of the binding mode of p300 co-substrate to that of PCAF and HAT1; (c) A comparsion of tertiary structures revealed that the key residues Arg1410, Thr1411, and Trp1466 are the specific residues of p300.

Table S1. Chemical structures of the 110 natural compounds selected as potential P300 inhibitors.

ID	Commerical ID	Company	Chemical Structure
1	NP-001578	AnalytiCon Discovery NP	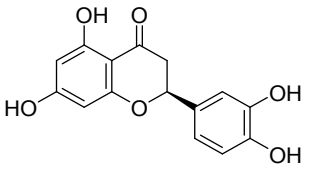
2	NP-003704	AnalytiCon Discovery NP	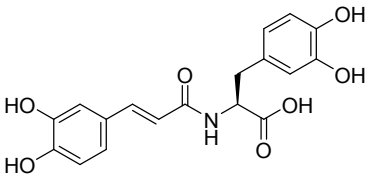
3	NP-000087	AnalytiCon Discovery NP	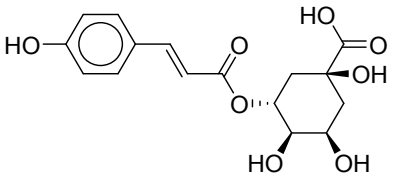
4	NP-001571	AnalytiCon Discovery NP	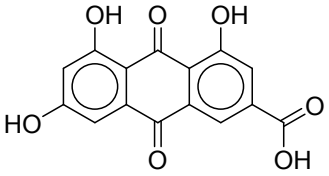
5	NP-010776	AnalytiCon Discovery NP	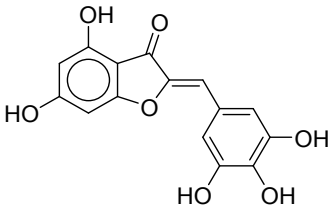
6	NP-001788	AnalytiCon Discovery NP	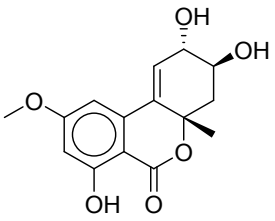
7	NP-003317	AnalytiCon Discovery NP	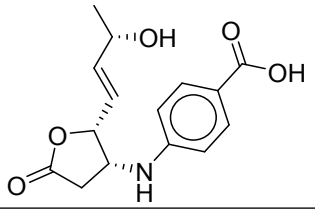

8	NP-006189	AnalytiCon Discovery NP	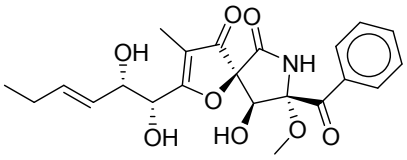
9	NP-001782	AnalytiCon Discovery NP	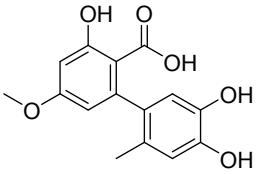
10	NP-002124	AnalytiCon Discovery NP	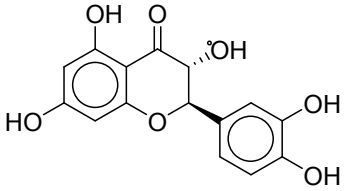
11	NP-009048	AnalytiCon Discovery NP	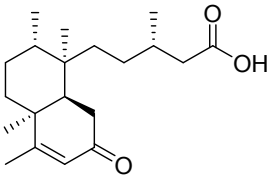
12	NP-002803	AnalytiCon Discovery NP	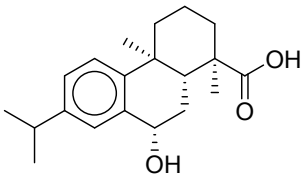
13	NP-001787	AnalytiCon Discovery NP	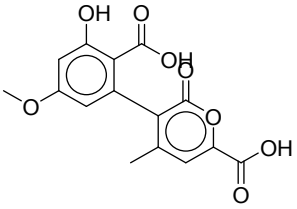
14	NP-015003	AnalytiCon Discovery NP	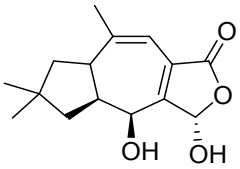
15	NP-006592	AnalytiCon Discovery NP	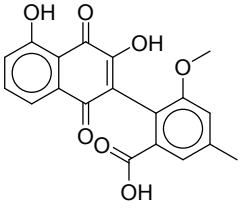
16	NP-000961	AnalytiCon Discovery NP	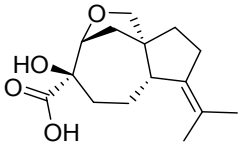

17	NP-009004	AnalytiCon Discovery NP	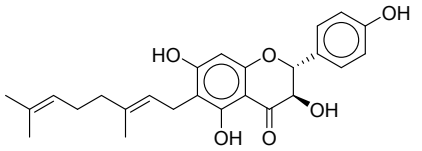
18	NP-001002	AnalytiCon Discovery NP	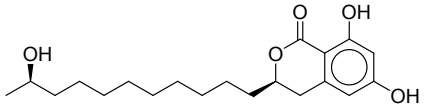
19	NP-014517	AnalytiCon Discovery NP	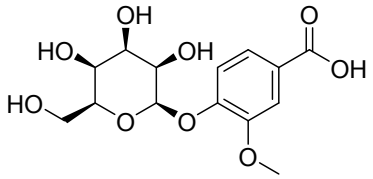
20	NP-002298	AnalytiCon Discovery NP	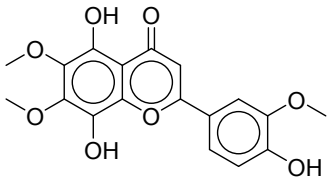
21	NP-000226	AnalytiCon Discovery NP	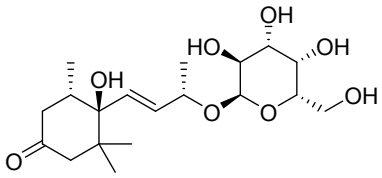
22	NP-000118	AnalytiCon Discovery NP	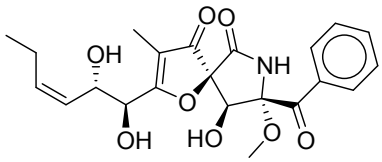
23	NP-001017	AnalytiCon Discovery NP	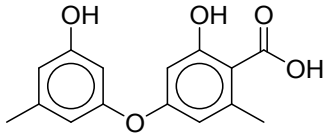
24	NP-003582	AnalytiCon Discovery NP	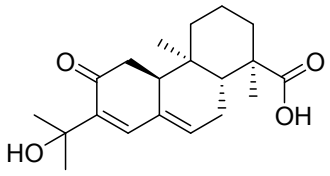
25	NP-015134	AnalytiCon Discovery NP	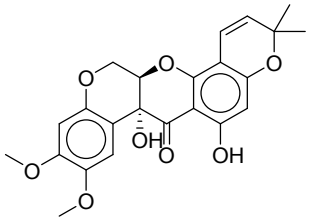

26	NP-015003	AnalytiCon Discovery NP	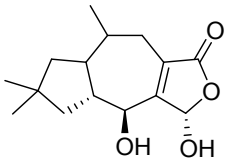
27	NP-018492	AnalytiCon Discovery NP	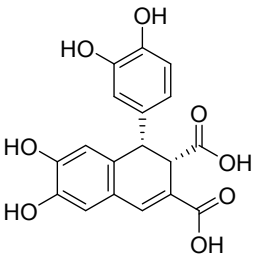
28	NP-001946	AnalytiCon Discovery NP	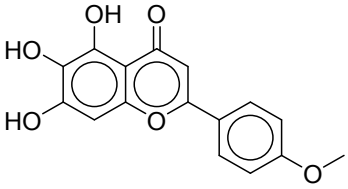
29	NP-016399	AnalytiCon Discovery NP	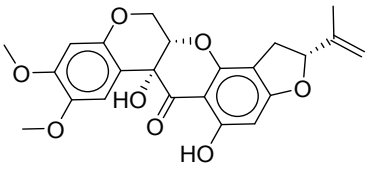
30	NP-001409	AnalytiCon Discovery NP	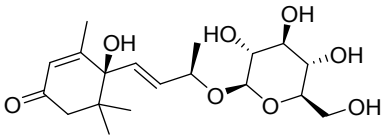
31	NP-001781	AnalytiCon Discovery NP	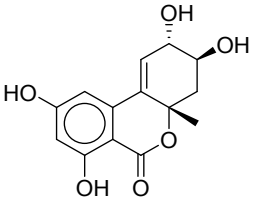
32	NP-002092	AnalytiCon Discovery NP	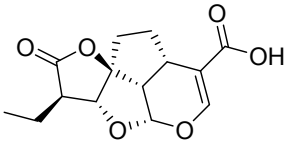
33	NP-003111	AnalytiCon Discovery NP	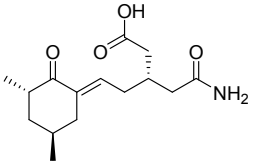
34	NP-007872	AnalytiCon Discovery NP	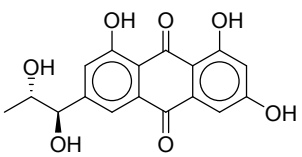

35	NP-014114	AnalytiCon Discovery NP	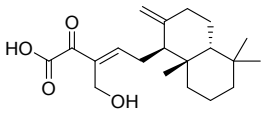
36	NP-000334	AnalytiCon Discovery NP	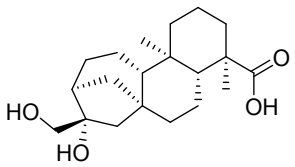
37	NP-003108	AnalytiCon Discovery NP	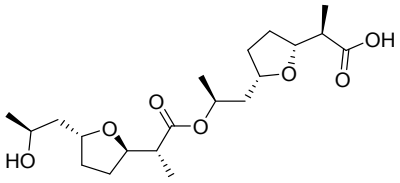
38	NP-001210	AnalytiCon Discovery NP	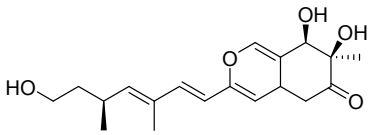
39	NP-010468	AnalytiCon Discovery NP	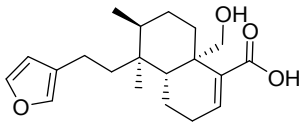
40	NP-003582	AnalytiCon Discovery NP	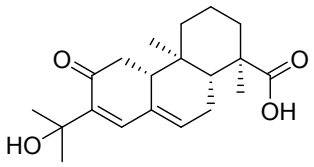
41	NP-017061	AnalytiCon Discovery NP	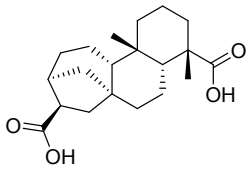
42	NP-006891	AnalytiCon Discovery NP	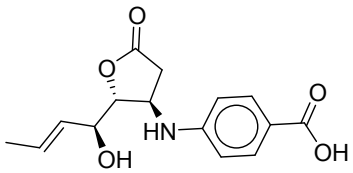
43	NP-018849	AnalytiCon Discovery NP	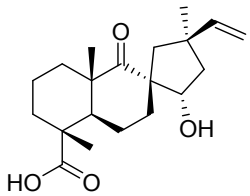
44	C-002	Indofine NP	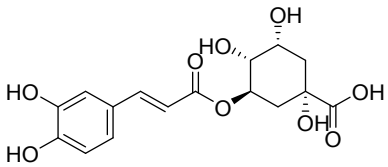

45	A-003	Indofine NP	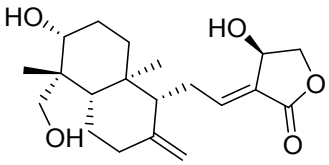
46	NS_009304	Princeton NP	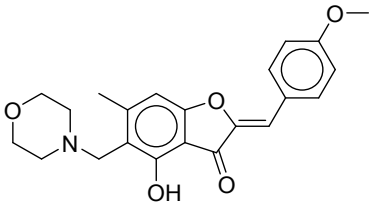
47	NS_012847	Princeton NP	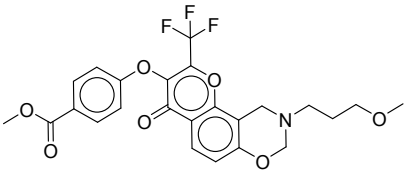
48	NS_012735	Princeton NP	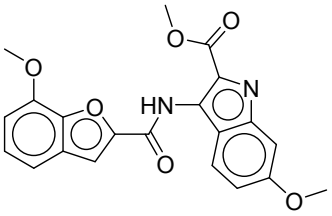
49	NS_012902	Princeton NP	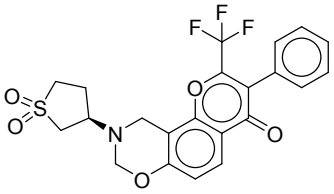
50	NS_007019	Princeton NP	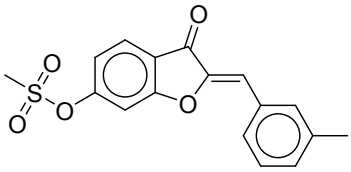
51	NS_004515	Princeton NP	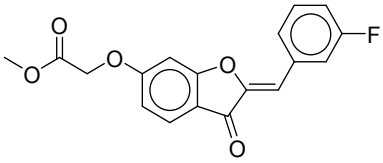
52	NS_003027	Princeton NP	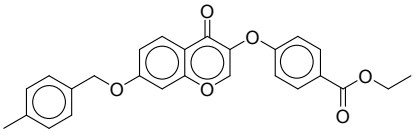
53	NS_001080	Princeton NP	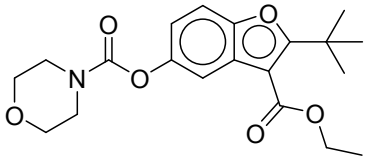

54	NS_001465	Princeton NP	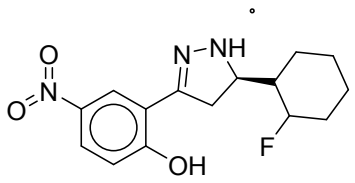
55	NS_003799	Princeton NP	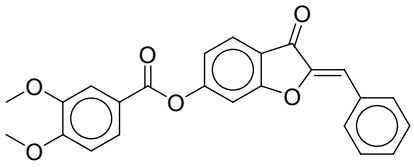
56	NS_005509	Princeton NP	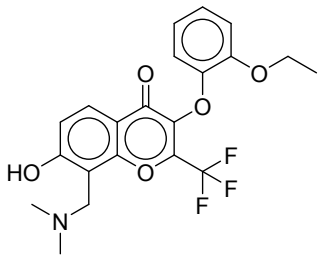
57	NS_007010	Princeton NP	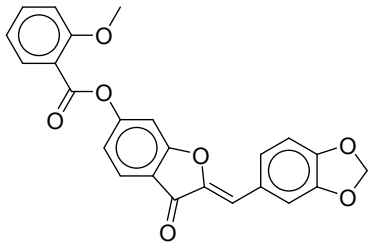
58	NS_004350	Princeton NP	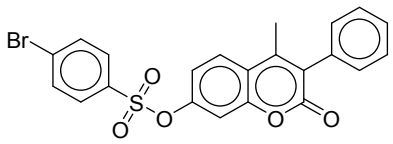
59	NS_010447	Princeton NP	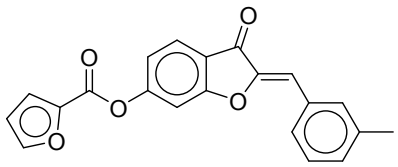
60	NS_004838	Princeton NP	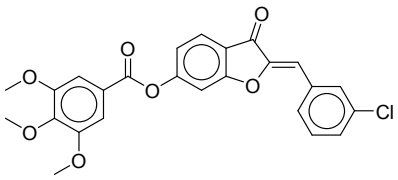
61	NS_007929	Princeton NP	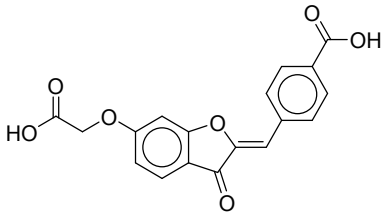

62	NS_011546	Princeton NP	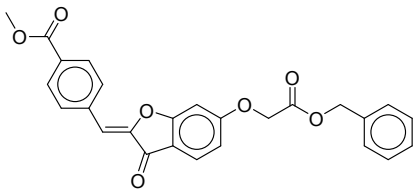
63	NS_009436	Princeton NP	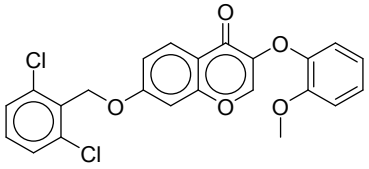
64	NS_010723	Princeton NP	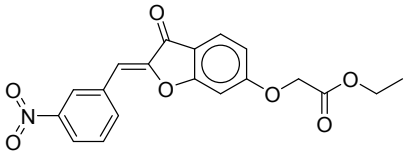
65	NS_012328	Princeton NP	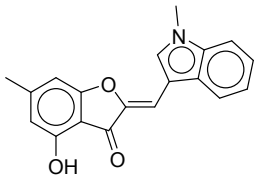
66	NS_012385	Princeton NP	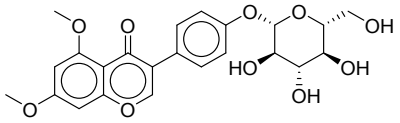
67	NS_007238	Princeton NP	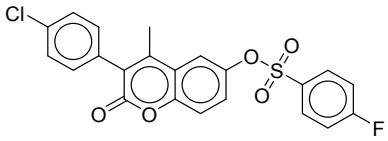
68	NS_012798	Princeton NP	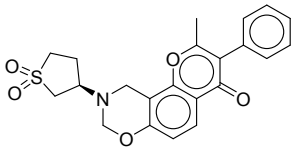
69	NS_012947	Princeton NP	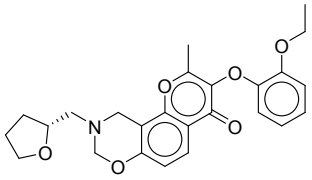
70	NS_003416	Princeton NP	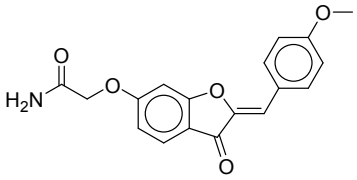

71	NS_006044	Princeton NP	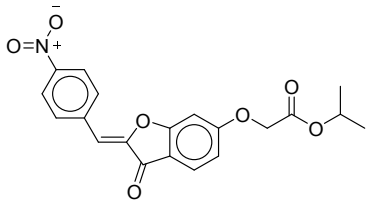
72	NS_003428	Princeton NP	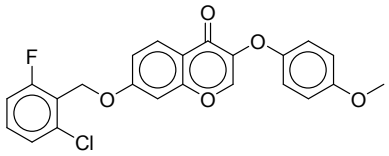
73	NS_004586	Princeton NP	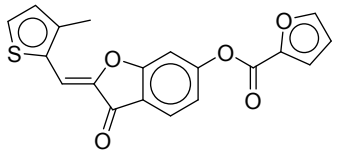
74	NS_005096	Princeton NP	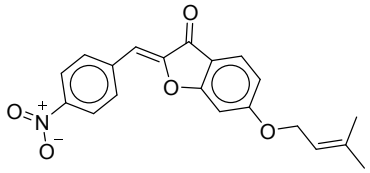
75	NS_006662	Princeton NP	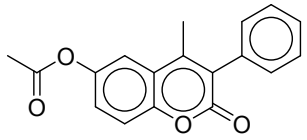
76	NS_005107	Princeton NP	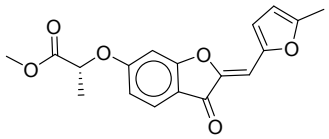
77	NS_002770	Princeton NP	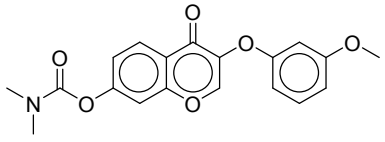
78	NS_002895	Princeton NP	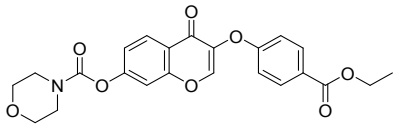
79	NS_001475	Princeton NP	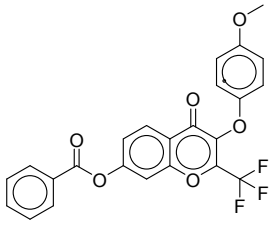
80	NS_000584	Princeton NP	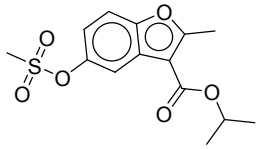

81	NS_004385	Princeton NP	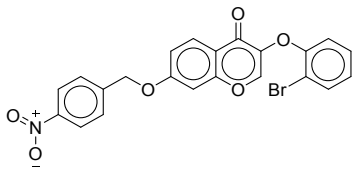
82	NS_004824	Princeton NP	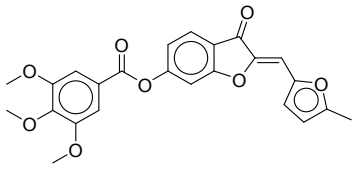
83	NS_003998	Princeton NP	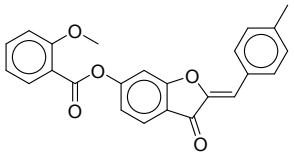
84	NS_001203	Princeton NP	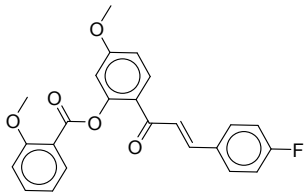
85	NS_007210	Princeton NP	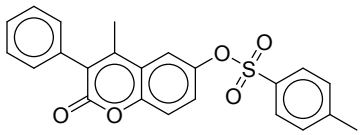
86	NS_007077	Princeton NP	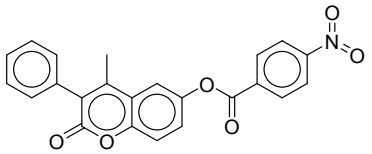
87	NS_007695	Princeton NP	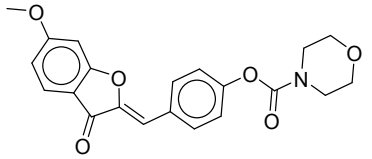
88	NS_009435	Princeton NP	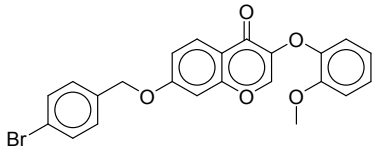
89 (**NP-1**)	AG-690/12884009	Specs NP	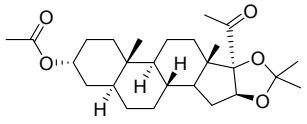
90 (**NP-2**)	AP-123/40765218	Specs NP	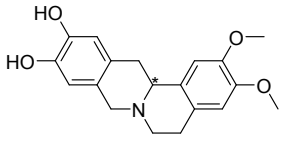

91 (**NP-3**)	AE-508/43280806	Specs NP	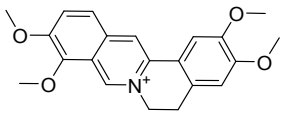
92 (**NP-4**)	AH-214/21165033	Specs NP	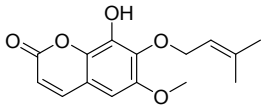
93 (**NP-5**)	AK-693/43417390	Specs NP	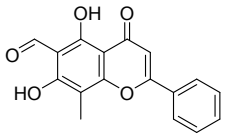
94 (**NP-6**)	AM-721/20681006	Specs NP	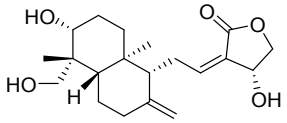
95 (**NP-7**)	AA-504/21163113	Specs NP	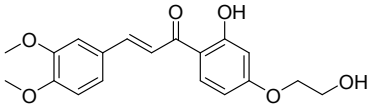
96 (**NP-8**)	AO-774/41465395	Specs NP	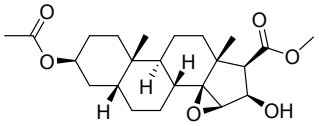
97 (**NP-9**)	AK-693/43417378	Specs NP	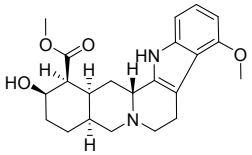
98 (**NP-10**)	AK-198/11618045	Specs NP	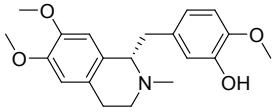
99 (**NP-11**)	AO-229/41747043	Specs NP	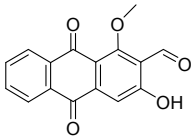
101 (**NP-12**)	AO-774/41465517	Specs NP	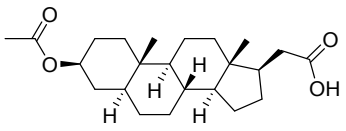
102 (**NP-13**)	AE-848/21020030	Specs NP	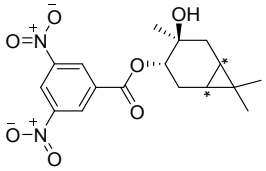

103 (**NP-14**)	AC-776/41252595	Specs NP	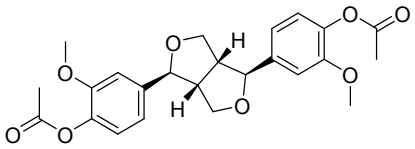
105 (**NP-15**)	AO-222/41148896	Specs NP	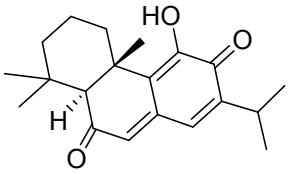
106	AH-034/21082028	Specs NP	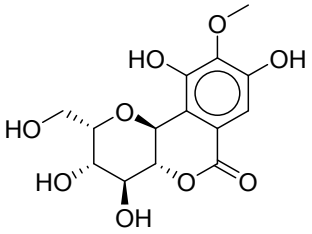
107	AA-504/07224047	Specs NP	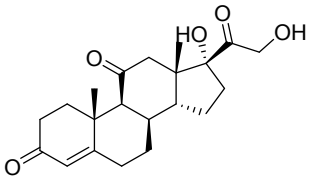
108	AO-222/41148787	Specs NP	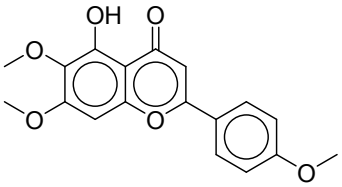
109	AC-542/20643018	Specs NP	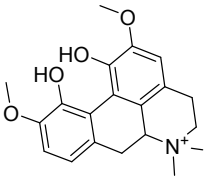
110	AH-034/11107027	Specs NP	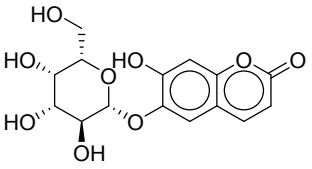

Table S2. The inhibitory potencies (IC_{50}) of **NP-2**, **NP-3**, **NP-9**, and **NP-15** against eight types of human cancer cell lines.[a]

Cancer cell line	Cancer type	IC_{50} (μM)			
		NP-2	**NP-3**	**NP-9**	**NP-15**
MDA-MB-231	Triple-negative breast cancer	50-100	>200	>100	11.63
ZR-75-1	Breast cancer	41.09	12.87	>100	2.323
LNCaP	Prostate cancer	50-100	100-200	>100	15.65
DU 145	Prostate cancer	>200	>200	>100	29.98
PANC-1	Pancreatic cancer	100	>200	>100	9.254
HCT 116	Colon cancer	100	100-200	>100	11.81
DLD-1	Colon cancer	>200	>200	>100	6.032
SH-SY5Y	Neuroblastoma	>200	>200	>100	13.21

[a] The inhibitory activity was determined by cell viability assays as described in Supporting Information Experimental Methods.

Reference:

1. Li, G.-B.; Yang, L.-L.; Wang, W.-J.; Li, L.-L.; Yang, S.-Y. ID-Score: a new empirical scoring function based on a comprehensive set of descriptors related to protein–ligand interactions. *J. Chem. Inf. Model.* 2013, **53**, 592-600.

2. Lau, O. D.; Kundu, T. K.; Soccio, R. E.; Ait-Si-Ali, S.; Khalil, E. M.; Vassilev, A.; Wolffe, A. P.; Nakatani, Y.; Roeder, R. G.; Cole, P. A. HATs off: selective synthetic inhibitors of the histone acetyltransferases p300 and PCAF. *Mol. Cell* 2000, **5**, 589-595.

3. Hao, J.; Ao, A.; Zhou, L.; Murphy, C. K.; Frist, A. Y.; Keel, J. J.; Thorne, C. A.; Kim, K.; Lee, E.; Hong, C. C. Selective small molecule targeting β-catenin function discovered by in vivo chemical genetic screen. *Cell Rep.* 2013, **4**, 898-904.

4. Yang, H.; Pinello, C. E.; Luo, J.; Li, D.; Wang, Y.; Zhao, L. Y.; Jahn, S. C.; Saldanha, S. A.; Planck, J.; Geary, K. R. Small-molecule inhibitors of acetyltransferase p300 identified by high-throughput screening are potent anticancer agents. *Mol. Cancer Ther.* 2013, **12**, 610-620.

5. Holzhauser, S.; Freiwald, A.; Weise, C.; Multhaup, G.; Han, C. T.; Sauer, S. Discovery and Characterization of Protein‐Modifying Natural Products by MALDI Mass Spectrometry Reveal Potent SIRT1 and p300 Inhibitors. *Angew. Chem. Int. Edit.* 2013, **52**, 5171-5174.

6. Sun, Y.; Jiang, X.; Chen, S.; Price, B. D. Inhibition of histone acetyltransferase activity by anacardic acid sensitizes tumor cells to ionizing radiation. *FEBS Lett.* 2006, **580**, 4353-4356.

7. Balasubramanyam, K.; Altaf, M.; Varier, R. A.; Swaminathan, V.; Ravindran, A.;

Sadhale, P. P.; Kundu, T. K. Polyisoprenylated benzophenone, garcinol, a natural histone acetyltransferase inhibitor, represses chromatin transcription and alters global gene expression. *J. Biol. Chem.* 2004, **279**, 33716-33726.

8. Balasubramanyam, K.; Varier, R. A.; Altaf, M.; Swaminathan, V.; Siddappa, N. B.; Ranga, U.; Kundu, T. K. Curcumin, a novel p300/CREB-binding protein-specific inhibitor of acetyltransferase, represses the acetylation of histone/nonhistone proteins and histone acetyltransferase-dependent chromatin transcription. *J. Biol. Chem.* 2004, **279**, 51163-51171.

9. Ravindra, K. C.; Selvi, B. R.; Arif, M.; Reddy, B. A.; Thanuja, G. R.; Agrawal, S.; Pradhan, S. K.; Nagashayana, N.; Dasgupta, D.; Kundu, T. K. Inhibition of lysine acetyltransferase KAT3B/p300 activity by a naturally occurring hydroxynaphthoquinone, plumbagin. *J. Biol. Chem.* 2009, **284**, 24453-24464.

10. Zeng, F.; Peng, S.; Li, L.; Mu, L.; Zhang, Z.; Zhang, Z.; Huang, N. Structure-based identification of drug-like inhibitors of p300 histone acetyltransferase. *Acta Pharma. Sinica* 2013, **48**, 700-708.

11. Bowers, E. M.; Yan, G.; Mukherjee, C.; Orry, A.; Wang, L.; Holbert, M. A.; Crump, N. T.; Hazzalin, C. A.; Liszczak, G.; Yuan, H. Virtual ligand screening of the p300/CBP histone acetyltransferase: identification of a selective small molecule inhibitor. *Chem. Biol.* 2010, **17**, 471-482.

12. Dancy, B. M.; Crump, N. T.; Peterson, D. J.; Mukherjee, C.; Bowers, E. M.; Ahn, Y. H.; Yoshida, M.; Zhang, J.; Mahadevan, L. C.; Meyers, D. J. Live‐Cell Studies of p300/CBP Histone Acetyltransferase Activity and Inhibition. *Chembiochem* 2012, **13**,

2113-2121.

13. Tohyama, S.; Tomura, A.; Ikeda, N.; Hatano, M.; Odanaka, J.; Kubota, Y.; Umekita, M.; Igarashi, M.; Sawa, R.; Morino, T. Discovery and characterization of NK13650s, naturally occurring p300-selective histone acetyltransferase inhibitors. *J. Org. Chem.* 2012, **77**, 9044-9052.

14. Pei, J.; Kim, B.-H.; Grishin, N. V. PROMALS3D: a tool for multiple protein sequence and structure alignments. *Nucleic Acids Res.* 2008, **36**, 2295-2300.

15. Minami, S.; Sawada, K.; Chikenji, G. MICAN : a protein structure alignment algorithm that can handle Multiple-chains, Inverse alignments, C α only models, Alternative alignments, and Non-sequential alignments. *BMC Bioinformatics* 2013, **14**, 1-22.